



HAL
open science

Low-energy building envelope design in Lebanese climate context: the case study of traditional Lebanese detached house

Emilio Sassine, Joseph Dgheim, Yassine Cherif, Emmanuel Antczak

► To cite this version:

Emilio Sassine, Joseph Dgheim, Yassine Cherif, Emmanuel Antczak. Low-energy building envelope design in Lebanese climate context: the case study of traditional Lebanese detached house. *Energy efficiency*, 2022, 15 (8), pp.56. 10.1007/s12053-022-10065-6 . hal-03972263

HAL Id: hal-03972263

<https://univ-artois.hal.science/hal-03972263>

Submitted on 7 Feb 2023

HAL is a multi-disciplinary open access archive for the deposit and dissemination of scientific research documents, whether they are published or not. The documents may come from teaching and research institutions in France or abroad, or from public or private research centers.

L'archive ouverte pluridisciplinaire **HAL**, est destinée au dépôt et à la diffusion de documents scientifiques de niveau recherche, publiés ou non, émanant des établissements d'enseignement et de recherche français ou étrangers, des laboratoires publics ou privés.

Low-energy building envelope design in Lebanese climate context: The case study of traditional Lebanese detached house

Emilio SASSINE^{1,*}; Joseph DGHEIM¹; Yassine CHERIF²; Emmanuel ANTCZAK²

¹ Lebanese University, Habitat and Energy Unit, Group of Mechanical Thermal and Renewable Energies – Laboratory of Applied Physics (LPA-GMTER), Faculty of Sciences, FANAR 90656, Lebanon

² Univ. Artois, Univ. Lille, Institut Mines-Télécom, Junia, ULR 4515 – LGCgE, Laboratoire de Génie Civil et géo-Environnement, F-62400 Béthune, France

Abstract

This paper aims to analyze the thermal efficiency of a traditional Lebanese detached house in order to identify the effect of various geometric (Orientation and window size), thermophysical (insulation level and solar reflection level), and technical (air change rate) parameters on its energy performance in the four different climate conditions in Lebanon. Different scenarios are first selected for each parameter and compared with the Base Case; then a parametric analysis is performed to check the influence of each building parameter on the building thermal energy efficiency, the remaining parameters being unchanged. The parametric analysis is followed by a building optimization simulation for determining the optimal building configuration, and defining the main guidelines towards energy efficient building design in each climate context. Substantial thermal improvements of about 80% were reached between the Base Case and the Optimal Case in the four climate zones. The findings of the present work can be applied for new buildings as guidelines for optimal efficient design as well as in existing buildings to determine the best interventions and the potential savings.

Keywords

Thermal performance, Residential buildings, Energy simulation, Building optimization, Mediterranean context

*Corresponding author: Emilio SASSINE, Email address: emilio.sassine@gmail.com

NOMENCLATURE

<i>T</i>	Temperature (°C)
<i>A</i>	Area (m ²)
<i>Q</i>	Thermal energy demand (kWh)
<i>U</i>	Thermal transmittance (Wm ⁻² K ⁻¹)
<i>C</i>	Heat Capacity (J.m ⁻² .K ⁻¹)
<i>AC</i>	Rate of building air exchange (h ⁻¹)
<i>e</i>	Thickness (m)
<i>SHGC</i>	Solar Heat Gain Coefficient (-)
<i>BC</i>	Base Case
<i>RC</i>	Reinforced Concrete
<i>R</i>	Roof
<i>G</i>	Ground Floor
<i>W</i>	Wall
 <i>Greek letters</i>	
λ	Thermal conductivity (Wm ⁻¹ K ⁻¹)
ρ	Density (kgm ⁻³)
φ	Heat flux (Wm ⁻²)
 <i>Subscripts</i>	
<i>win</i>	Window
<i>tot</i>	Total
<i>eq</i>	Equivalent
<i>ins</i>	Thermal insulation
<i>N</i>	North direction
<i>S</i>	South direction
<i>E</i>	East direction
<i>W</i>	West direction

1 Introduction

Researchers worldwide are investigating building optimization methodologies for enhancing buildings' energy performance towards optimal passive designs especially for residential buildings. The energy needs in households mainly depend on the building envelope, the local climate, the HVAC systems, and the occupants' behavior.

Many scientific works adopted building energy optimization approaches either for determining the best energy saving measures for different existing buildings or for determining the optimal building design for new buildings. Among the most famous optimization methods, Genetic algorithms are used in many building optimization problems; they are based Darwin's "natural selection" concept in biological evolution to generate optimal solutions [1]. Salata et al. [2] used the genetic algorithms and building energy simulations using a residential building case study to determine the most advantageous retrofitting interventions for nineteen different European cities. Bucking et al. [3] determined two optimal approaches for building passive design: the first approach included super insulated walls with small window areas, and the second design is based on lower thermal insulation thickness and appropriately sized windows in the South direction for passive solar gains. The two approaches were found to be valid for achieving the Net-Zero Energy performance. Chvatal et al. [4] assessed the impact of increasing the building envelope insulation on the summer thermal discomfort and the needs for air-conditioning. The results showed that adding insulation should be accompanied by a control on solar gains and internal gains to avoid summer overheating. Ibrahim et al. [5] determined the optimal insulation thickness in the Lebanese coastal and inland climate zones using the genetic algorithm and the life cycle insulation cost of as objective function. The optimum thickness varied between 3 and 5 cm depending on the climate conditions and the wall orientation. Jin et al. [6] performed a free-form shape optimization to optimize the thermal performance of buildings in various climate zones using Rhinoceros Software and the genetic algorithm. Rosso et al. [7] used the genetic algorithm and the Pareto frontier to facilitate the selection of the best retrofit measures for a residential Italian building. The optimal measures were able to reduce by about 50% of the annual energy cost and CO₂ emissions. Wright et al. [8] divided the building envelope façade into small cells and used a multi-objective genetic algorithm to find the optimal fenestration configuration allowing to minimize the energy use and the investment cost. Their results led to optimal innovative architectural designs. Zhang et al. [9] also used the genetic algorithm to minimize heating and lighting energy use and summer discomfort, and maximize the Daylight Illuminance in school buildings in cold Chinese climate context.

In a country such as Lebanon where nearly 97% of energy needs are imported in the form of multiple petroleum products [10], the launching of Energy Efficiency and Renewable Energy projects is crucial. Some thermal insulation standards projects were launched for this purpose, such as the Lebanese Standard "NL 68: 1999" entitled "Guide of thermal insulation and thermal comfort in buildings" developed in collaboration with the CSTB France, and the "Thermal Standard for Buildings in Lebanon (2005 and 2010)" developed in the LEB/GEF/G35 project [11]. However, these approaches were limited to some basic building parameters such as the thermal transmission coefficients of the building envelope and neglected many other important parameters that can have a significant impact in the building design such as the solar absorption coefficients, the air change rate, the recommended building

orientation, and the glazed ratios. In addition, no limitations were defined for heating and cooling loads and no detailed calculation methods were presented. A lot of efforts are still to be invested for evaluating the thermal performance of Lebanese buildings and providing guidelines for energy efficiency measures for the design of new buildings or the retrofit of existing buildings.

The average area of dwellings in Lebanon is 129.3 m², and about 33% of them are detached individual houses [12]. 21.8% of homes are heated by electricity, 25% by oil, 27.3% by Gas (LPG), and 17.6% by wood or coal [12]. As for air conditioning, the main systems are electric fans and split air conditioners. The heating and cooling are estimated at about 45% of total residential energy consumption in the Lebanese context [12], although there are substantial discrepancies for heating and cooling needs throughout the country depending on the location. Heating and cooling needs in buildings should be prioritized in any plan aiming at moderating the increase in Lebanon's energy consumption and meeting the international obligations for reducing the CO₂ emissions. This plan must take into consideration both energy efficient design of the new buildings and adequate refurbishment of the existing ones.

The thermal performance of Lebanese buildings is still unknown and very few researches have examined the optimal building envelope parameters in the Lebanese context. This paper allows a better understanding of the thermal performance of Lebanese buildings through a scientific approach by investigating the optimal design in four different Lebanese climate zones. A thermal parametric analysis of a residential building case study and a building thermal optimization based on these parameters is here presented using the Genetic Algorithm optimization approach with GenOpt® Software. The algorithm process is based on the selection of the more performing parameters ("phenotypes") with respect to the objective solutions to be conveyed to the following parameters generation. The more performing parameters will thus progressively substitute the less performing ones converging towards the optimal set of parameters.

In the first part, the thermal performance of a specific building case study corresponding to the Lebanese traditional detached house typology is examined through a dynamic building thermal simulation using TRNSYS® Software [13] in the Lebanese climate context. The parameters having the most impact on the heating and cooling building energy needs are analyzed: the external climate (climate zone), the building orientation and the transparent surfaces 'size, the solar absorption level, the air change rate, and the thermal insulation level. The effect of these parameters on space heating and cooling in the different Lebanese climate zones is analyzed with respect to reference values considered for a "Base Case". Different scenarios are first selected for each parameter and compared with the Base Case; then a building optimization is performed to check the optimal value for each parameter on the building thermal energy efficiency, the remaining parameters being unchanged.

In the second part, a global building optimization investigation is performed on all the parameters simultaneously in order to find the best building configuration for optimal yearly energy needs, in each climate zone.

2 Methodology and building case study

The studied building is a 150 m² typical Lebanese detached house consisting of two floors (10.5m x 7.15m each) as shown in Fig. 1.

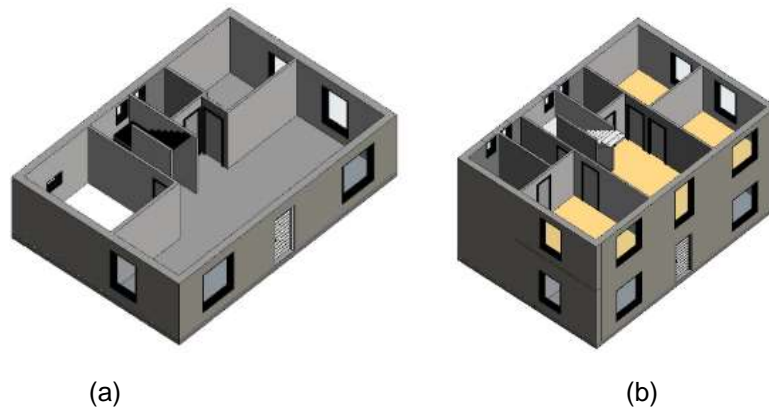


Figure 1- First floor (a) and second floor (b) 3D views of the studied building

The thermal properties of the masonry walls made of hollow blocks and mortar joints were determined experimentally while the remaining thermal properties of the building envelope materials were determined from literature and are reported in Table 1.

Table 1- Thermophysical properties of the materials accounted in the simulated building [13]

Materials	Conductivity λ (W/mK)	Density ρ (kg/m ³)	Specific heat c_p (J/kgK)
Polystyrene insulation	0.04	40	800
Concrete	2.10	2400	800
Plaster and Mortar	1.41	1863	1077
Stone cladding and tiling	3.00	2500	1000

When it comes to openings, double glazed windows were used with a U-value of 2.95 W/m²K and a g-value of 0.777; one solid wooden door (1m x 2.2m) was considered at the Southern façade with a U-value of 2.5 W/m²K [13].

The composition of the building envelope components is reported in Table 2.

Table 2- Envelope composition (from outside to inside) of the Base Case simulated building

Component	Layers (Ext-Int)	Thickness (cm)
Wall	Stone cladding	2
	Cement plaster	1
	Hollow block	15
	Cement plaster	1
Roof	RC slab	27
	Cement plaster	1
Ground floor	RC slab	30
	Mortar	2
	Stone tiling	2
Glazing	Double glazing	0.4 – 1.6 – 0.4
Door	Wooden door	4

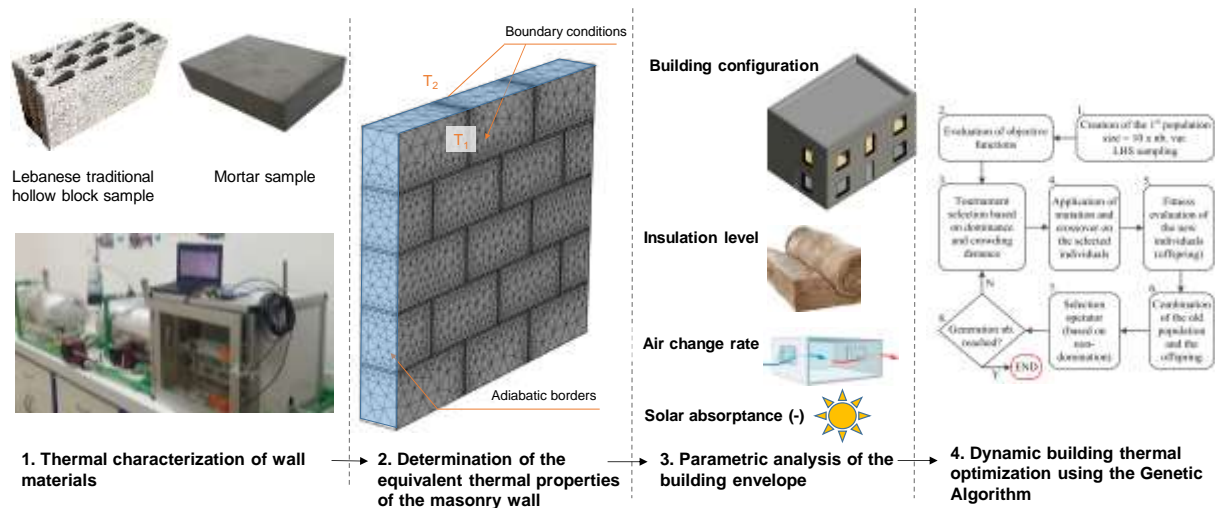


Figure 2- Adopted methodology

A schematic representation of the adopted methodology is presented in Fig. 2.

First, the thermal characterization of the hollow block and the mortar joint is performed thanks to an experimental thermal characterization setup using the fluxmetric method. The equivalent thermal properties of the masonry wall are then numerically computed using the numerical FEM method and the respective experimental thermal properties of blocks and mortar.

After determining the thermal properties of the hollow block and the mortar joint and evaluating the equivalent thermal properties of the masonry walls, the thermal performance of a Lebanese traditional detached house typology was investigated in two steps:

- A parametric analysis is then realized by examining the influence of the building parameters on the thermal energy performance of a traditional Lebanese building; these parameters include the building orientation, the transparent surfaces' size, the solar absorption level, the air change rate, and the thermal insulation level. The effects of the different building parameters on space heating and cooling energy needs in the different Lebanese climate zones were first analyzed and compared with respect to reference "Base Case" values. The impact of each parameter on the yearly building total thermal energy needs of the Base Case was also evaluated.
- A global building optimization was then performed by varying all the parameters simultaneously in order to find the best building configuration for optimal yearly energy needs, in each climate zone. This optimization made it possible to find the best building configuration for the different climate zones and end up with some interesting recommendations for energy efficient Lebanese buildings designs.

The optimization was performed using the GenOpt® optimization program for the minimization of the building energy needs. The cooling and heating energy needs were considered as cost function in the optimization algorithm and were evaluated by the Building energy simulation module in TRNSYS®. The coupling between GenOpt and TRNSYS® made it possible to vary building parameters considering them as variables with lower and upper bounds and optimize the building parameters for reaching the best building configuration by maximizing or minimizing pre-defined objective functions.

3 Thermal characterization of the hollow block wall

In this section a special attention is given to the experimental thermal characterization of the Lebanese traditional hollow block masonry wall for three main reasons:

- 1- These walls are specific to the Lebanese constructions and present an unexploited potential of investigation and understanding.
- 2- The masonry walls are made of two main components, the blocks and the joints; their equivalent thermal properties are thus complex to be determined.
- 3- The traditional masonry hollow block wall configuration will be used to validate heat transfer model used by the building energy simulation software by comparing the heat flux across the wall with the heat flux obtained by the FEM method using COMSOL Multiphysics® Software.

3.1 Experimental setup

The masonry hollow block that is one of the most common materials used in Lebanese constructions, it has a specific configuration typical of the region (Fig. 1). It has a length of 40 cm, a height of 20 cm, and different thicknesses varying between 10 and 30 cm. The sample used in the experimental testing procedure is 10 cm thick because the bigger the thickness is, the lower is the thermal heat flux through the wall, and thus the less precise are the measurements.

An experimental thermal characterization setup is used to determine the thermal properties (thermal conductivity and heat capacity) of building samples using the guarded hot plate method (Fig. 3). The lateral faces of the sample were covered with an insulation material to impose unidirectional heat transfer conditions. An imposed temperature boundary condition was applied on the sample sides. The temperatures and heat fluxes on both sides of the sample were simultaneously recorded through two thermocouples T-type and two tangential gradient fluxmeters having an active surface of $0.15 \times 0.15 \text{ m}^2$. This allows the determination of the thermal conductivity λ ($\text{W}\cdot\text{m}^{-1}\cdot\text{K}^{-1}$) and the specific heat c_p ($\text{J}\cdot\text{kg}^{-1}\cdot\text{K}^{-1}$) using the following calculation method [14].

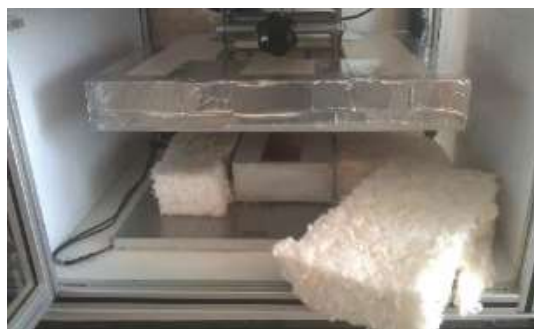


Figure 3- Thermal characterization device for building materials

3.2 Characterization method

3.2.1 Determination of the thermal conductivity

The sample is subjected to a temperature gradient ΔT (K) which generates a heat flux transfer ϕ ($\text{W}\cdot\text{m}^{-2}$) from the hot side to the cold one. When reaching the steady state condition, the heat flux at the upper

face of the sample φ_{sup} equals the heat flux at the bottom face of the sample φ_{inf} . The Fourier's law in unidirectional steady state conditions gives:

$$\varphi_{\text{sup}} = \varphi_{\text{inf}} = \frac{\Delta T}{R} \quad (1)$$

The thermal conductivity λ ($\text{W}\cdot\text{m}^{-1}\cdot\text{K}^{-1}$) can thus be determined from the thermal resistance R ($\text{m}^2\cdot\text{K}\cdot\text{W}^{-1}$) and the sample thickness e (m):

$$\lambda = \frac{e}{R} \quad (2)$$

3.2.2 Determination of the specific heat

Starting from a stable initial steady state, a temperature variation is imposed by changing the set point on one or both sample faces. The average initial temperature of the sample ($\Sigma T/2$), as well the fluxes over each side, will change to a new stable state with a new final average temperature ($\Sigma T_f/2$). The heat energy Q ($\text{J}\cdot\text{m}^{-2}$) that is stored (or released) during this transition can be related to the heat fluxes difference ($\Delta\varphi$) according to the relation:

$$Q = \int_{t_i}^{t_f} \Delta\varphi \cdot dt \quad (3)$$

The exchanged heat energy is also related to the initial and final average temperatures $\Sigma T/2$ and ΣT_f :

$$Q = C \times \frac{\Sigma T_f - \Sigma T_i}{2} \quad (4)$$

The sample's heat capacity C ($\text{J}\cdot\text{m}^{-2}\cdot\text{K}^{-1}$) is thus deduced from Eq. (3) and (4):

$$C = \frac{2 \times \int_{t_i}^{t_f} \Delta\varphi \cdot dt}{\Sigma T_f - \Sigma T_i} \quad (5)$$

The specific heat of the sample c_p ($\text{J}\cdot\text{kg}^{-1}\cdot\text{K}^{-1}$) can thus be deduced, knowing its density and thickness:

$$c_p = \frac{C}{\rho e} \quad (6)$$

3.2.3 Experimental results

A hollow block ($20 \times 40 \times 10 \text{ cm}^3$) and a parallelepiped molded mortar sample ($17 \times 23 \times 7.5 \text{ cm}^3$) were tested and their respective thermal properties were determined using Eq. 1-6 and the experimental measurement results (Fig. 4 and Fig. 5).

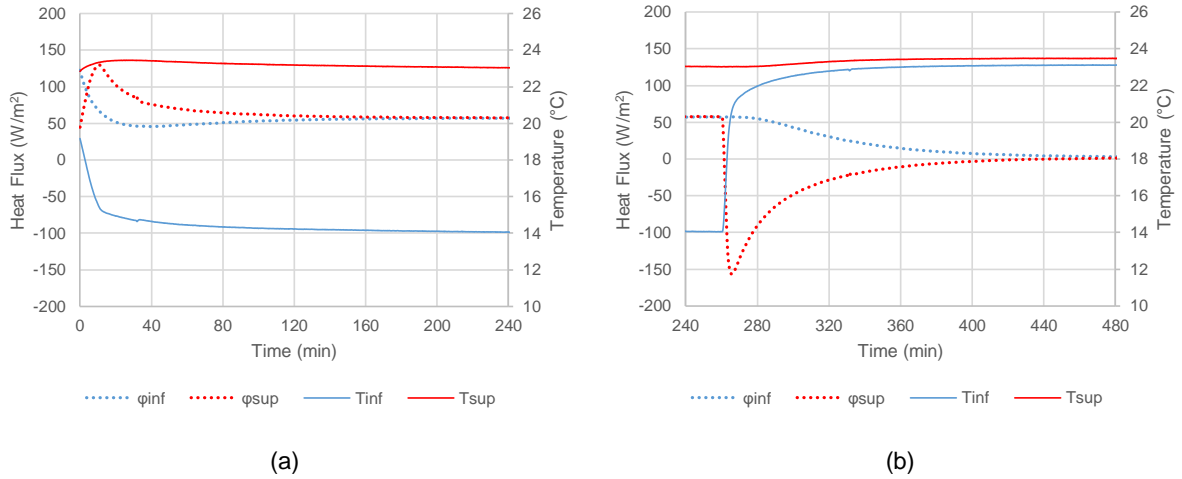


Figure 4- Experimental measurements for determining the thermal conductivity λ ($\text{W}\cdot\text{m}^{-1}\cdot\text{K}^{-1}$) (a) and the specific heat c_p ($\text{J}\cdot\text{kg}^{-1}\cdot\text{K}^{-1}$) for the hollow block sample (b)

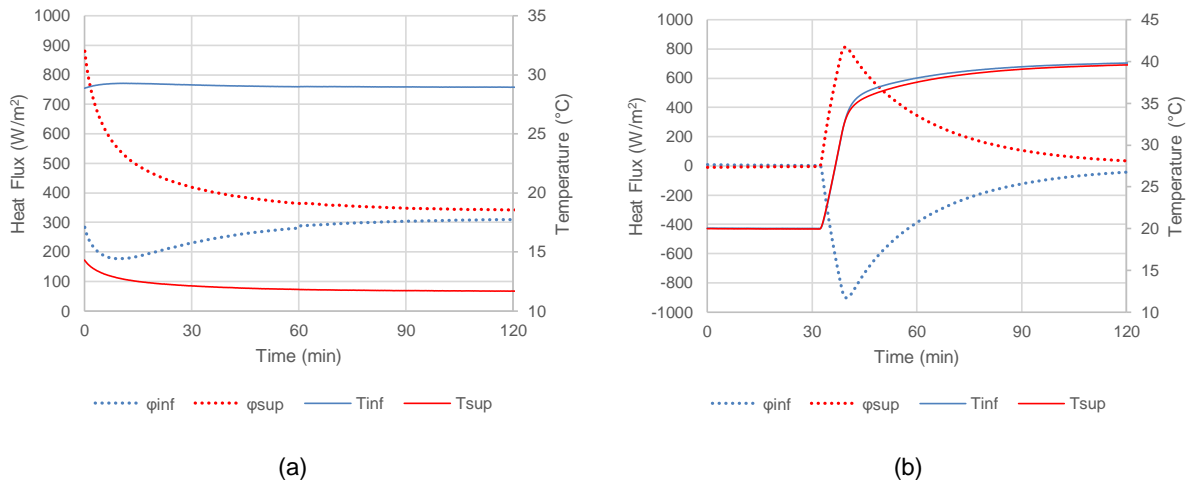


Figure 5- Experimental measurements for determining the thermal conductivity λ ($\text{W}\cdot\text{m}^{-1}\cdot\text{K}^{-1}$) and the specific heat c_p ($\text{J}\cdot\text{kg}^{-1}\cdot\text{K}^{-1}$) for the molded mortar sample

For the case of the hollow block sample, the hot sample side is maintained at 23°C while the cold side temperature is maintained at 14°C until reaching the steady state condition after about three hours (180 min) for determining the thermal conductivity. For determining the specific heat of the hollow block sample, the hot side of the heating plate is maintained at a constant temperature of 23°C while the cold plate is heated from an initial steady state of 14°C to a final steady state of 23°C .

Similarly, in the case of the mortar sample, the hot sample side is maintained at 29°C while the cold side temperature is maintained at 12°C until reaching the steady state condition after about one hour (60 min) for determining the thermal conductivity. For determining the specific heat of the mortar sample, the two heating plates are heated from an initial steady state of 19°C to a final steady state of 40°C .

The thermal properties of the tested samples are reported in Table 3.

Table 3- Experimental thermophysical properties of concrete hollow block and mortar joints

Material	Density (kg.m ⁻³)	Thermal conductivity (W.m ⁻¹ .K ⁻¹)	Specific heat (J.kg.K ⁻¹)
Mortar	1863	1.41	1077
Hollow block	1477	0.63	836

3.3 Determination of the thermal properties of the equivalent masonry walls

The investigated masonry wall is 15 cm thick and is made of two main components: the hollow blocks and the mortar joints used to glue these blocks and give structural rigidity to the walls. It is therefore essential to determine the equivalent thermal properties of this wall in order to be able to use it in the buildings thermal simulation software where the building layers should be inserted as uniform homogeneous layers.

The wall was modelled and simulated using the Finite Element Method (FEM) in COMSOL Multiphysics® with two different boundary conditions (Fig. 2) for defining its equivalent thermal capacity $(\rho c_p)_{eq}$ and its equivalent thermal conductivity λ_{eq} :

- Stationary study: $T_1= 40\text{ °C}$, $T_2= 20\text{ °C}$
- Time dependent simulation: initial temperature: 20 °C , boundary conditions: $T_1=T_2= 40\text{ °C}$.

The equivalent thermal conductivity λ_{eq} is thus calculated from Eq. 1 and Eq. 2 based on the numerical computed average heat flux on the wall in the stationary simulation study. The steady state heat flux obtained for a temperature difference of 20 °C is 90 W.m^{-2} , the equivalent resistance of the wall is $0.222\text{ W.m}^{-2}\text{.K}^{-1}$, and the equivalent thermal conductivity is $0.675\text{ W.m}^{-1}\text{.K}^{-1}$.

The equivalent thermal capacity $(\rho c_p)_{eq}$ is determined using Eq. 5 and Eq. 6 based on the numerical computed heat flux in the time dependent simulation study for the hollow block masonry wall and is found equal to $1\,250\,000\text{ J.m}^{-3}\text{.K}^{-1}$.

It is important to note that the equivalent thermal properties λ_{eq} and $(\rho c_p)_{eq}$ are just theoretical equivalent values that are used as input parameters in the building simulation software to represent the wall made of masonry blocks and mortar joints.

4 Thermal efficiency analysis

4.1 Climate context and simulation assumptions

Lebanon is a 10452 square kilometers country located on the eastern edge of the Mediterranean Sea. Despite its small area, it has a very rich topography making weather conditions vary widely from one place to another. The narrow Lebanese coast is heavily urbanized and contains the major cities; it is hot and humid in the summer, and a moderately cold winter with heavy rainfalls between January and March. The Mount Lebanon range is parallel to the coastline and reaches about 3000 meters; it has a typically Alpine climate, with rain, snow and subzero peak temperatures during winter. The Bekaa plateau has a drier climate and more pronounced temperature extremes. The Anti-Lebanon mountain range is parallel to the Bekaa and forms a natural eastern boundary from North to South between Lebanon and Syria.

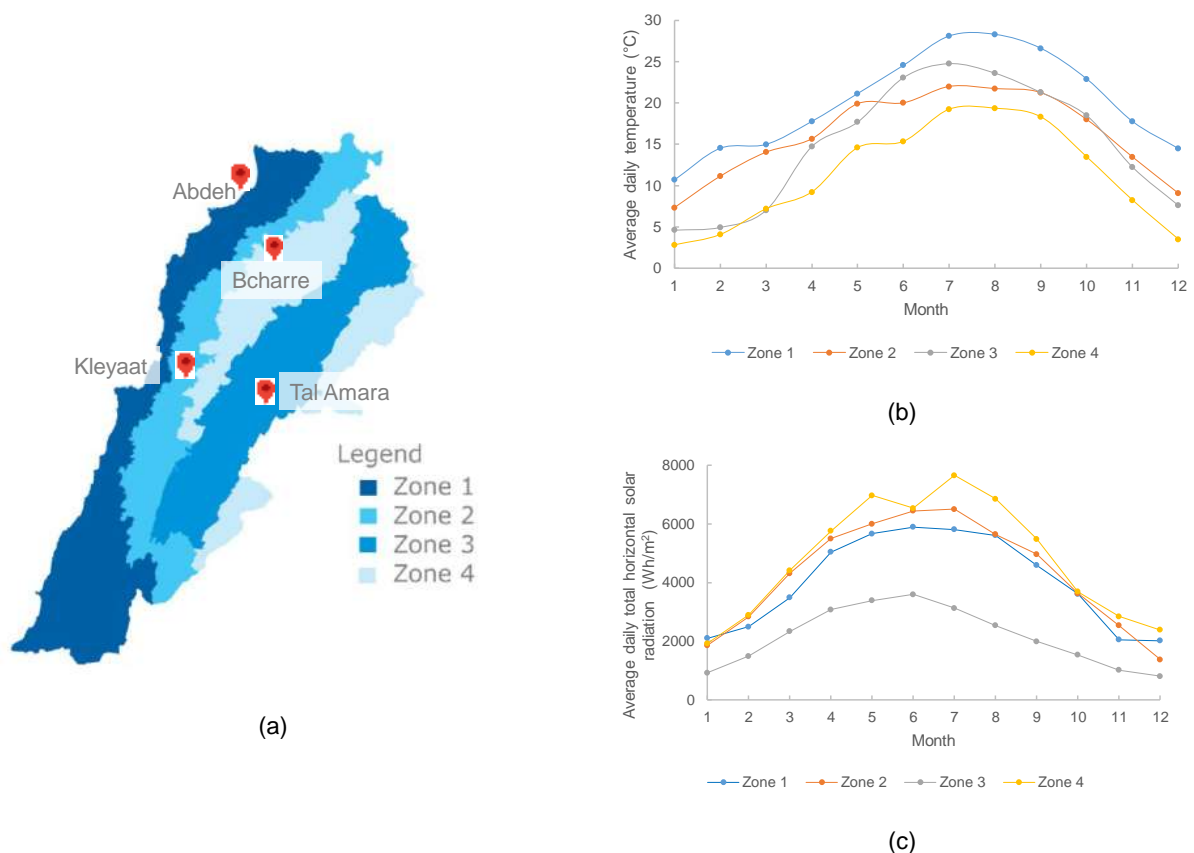


Figure 6- Climate zones in Lebanon (a), average daily temperature per month (b) and average daily horizontal solar radiation per month (c)

Four different climate zones are identified by the Thermal Standards for Buildings in Lebanon [11]: the coastal zone (Zone 1), the western mid-mountain Zone (Zone 2), the inland plateau (Zone 3), and the high mountain zone (Zone 4). In this study, four different locations belonging to the four different climate zones were selected for the simulations; their respective locations are shown in Fig. 6a.

The establishment of reliable TMY climate files for the selected locations was created based on weather parameters measurements provided by the Lebanese Agricultural Research Institute [15].

The average daily temperature per month as well as the average daily horizontal solar radiation per month, for the four chosen locations, are shown in Fig. 6b and Fig. 6c respectively.

TRNSYS® Software was used for dynamic building energy simulation. The Type 56 component was used to model the thermal behavior of the building using a pre-processing program, the TRNBUILD program for creating the so-called building file. The presence pattern has an important effect on energy consumption and this was recalled in many research works [16-19]. Since the objective of the present study is related to the investigation of the building envelope parameters, the occupancy was therefore assumed to be constant as reported in Table 4. A family of four people is considered and the occupancy is considered to be from 3 pm till 8 am in the weekdays and from 9 pm till 4 pm in the weekends. The internal gains due to people were selected according to the ISO 7730 norm with people considered at rest and the gains due to artificial lighting were considered to be 10 W/m². Thermal losses by transmission through thermal bridges were also neglected in the present study.

Table 4- Building occupancy

Day	Time	Occupancy (people)
Weekdays	00:00 – 08:00	4
	08:00 – 15:00	0
	15:00 – 24:00	4
Weekends	00:00 – 16:00	4
	16:00 – 21:00	0
	21:00 – 24:00	4

4.2 Heat transfer model validation

The heat transfer model used in the Type 56 module of TRNSYS® Software was compared to the heat transfer model provided by the Finite Element Method (FEM) used in COMSOL Multiphysics® Software in order to make sure that the 3D multilayered masonry wall is well represented in the 1D Building Simulation Software model.

A multilayered double wall was used for the model validation in order to validate the model in a relatively complex configuration (two non-symmetrical massive layers separated by an air gap); the wall is composed of two hollow block masonry layers separated by a 5 cm air gap as shown in Fig. 7, the wall is covered by an external cladding and internal plastering. The equivalent thermal properties of the HBW were used in the TRNSYS® BSM software with a total simulation duration of 800 hours (slightly more than one month).

The North wall was considered for the validation model and solar gains were removed by assuming a Sky factor equal to zero and internal gains as well as solar gains were also neglected for the model validation in order to simplify the boundary conditions as much as possible reducing them to the inside and outside wall temperatures T_{wi} and T_{wo} .

The validation was done by imposing the same temperatures T_{wi} and T_{wo} obtained from the Building Simulation Software on the 3D wall model and comparing the internal and external heat fluxes φ_i and φ_o between the Building Simulation Model (BSM) and the Finite Element Method (FEM) as shown in Fig. 8.

The comparison clearly shows that the FEM and the BSM provide very similar results for both internal and external heat fluxes ϕ_i and ϕ_o when applying the same wall surface temperatures T_{wi} and T_{wo} .

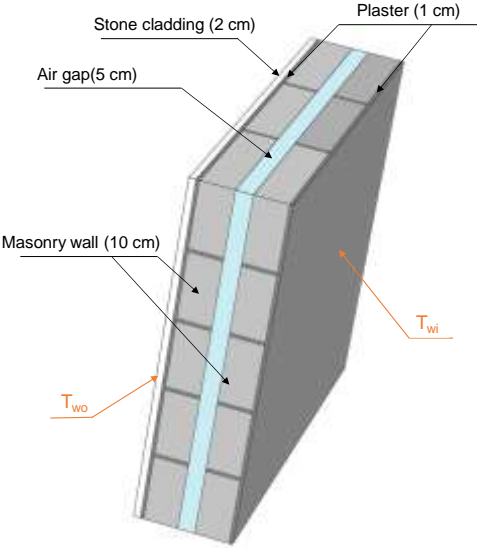


Figure 7- Simulated wall for model validation

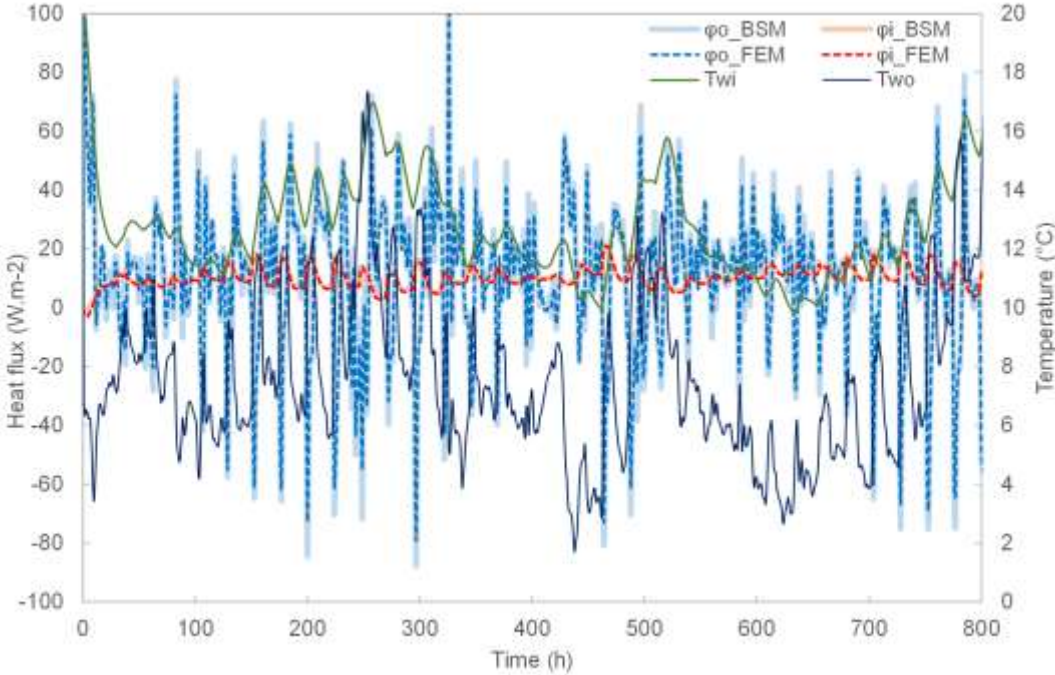


Figure 8- Comparison of the internal and external heat fluxes ϕ_i and ϕ_o between the FEM and the BSM

In order to define how well the measured and simulated heat fluxes are identical, the Nash-Sutcliffe Efficiency coefficient (NSE) [20] was used for ϕ_i and ϕ_o as shown in Fig. 9. It indicates how well the plot of measured versus simulated model data fits the 1:1 line. A value of $NSE=1$, corresponds to a perfect match of the model to the measurements; $NSE=0$, indicates that the model predictions are as accurate as the mean of the measurements data; and a negative value of NSE , indicates that the observed mean is a better predictor than the model. The results indicate a perfect match between the BSM and the FEM with NSE values close to 1 for both ϕ_i and ϕ_o and the heat transfer model used by the Building Simulation Software can thus be validated.

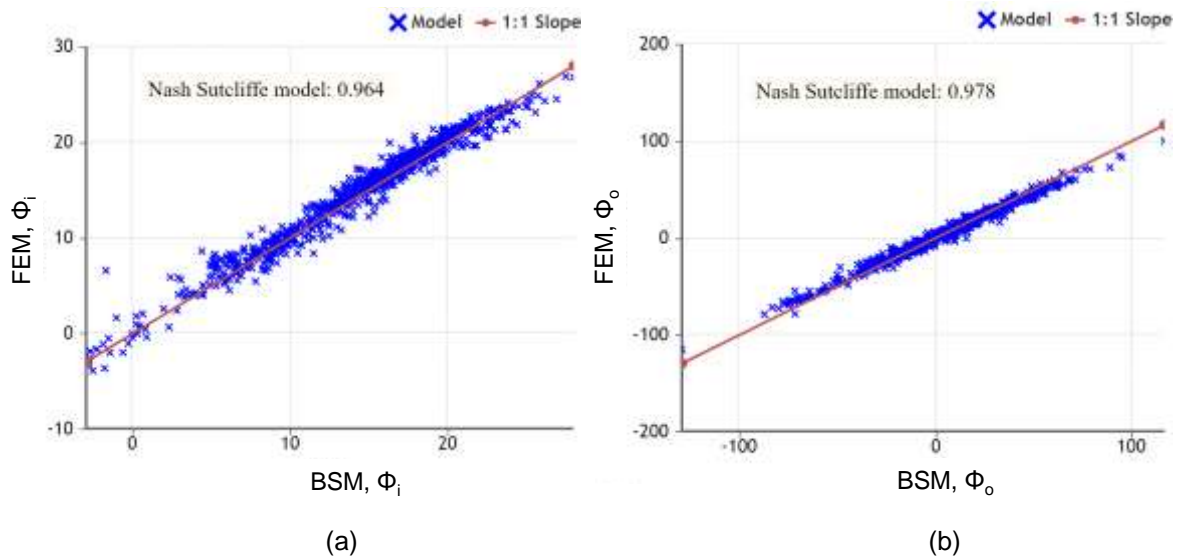


Figure 9- Nash Sutcliffe model for ϕ_i (a) and ϕ_o (b)

4.3 Investigation of the base case results

The base case includes medium values for each of the studied parameters: the building is South oriented with a total windows area of 30.38 m² (initial building design), the solar absorption level is 0.6 (medium darkness, light grey color) for the walls and the roof, the air change rate is 1 vol.h⁻¹ (reasonably tight house with an air change rate), the set temperatures are 20°C for heating and 24°C for cooling (average values recommended by the ASHRAE guidelines [21]), and no insulation is considered for the external walls.

The comparison of space heating and cooling for the Base Case in the four climate zones in Fig. 10a shows that cooling should be considered in zone 1 (coastal zone) with about 40 kWh/m²/yr while in the remaining zones the cooling load is relatively low with less than 20 kWh/m²/yr and can thus be neglected with respect to space heating.

On the other hand, the heating load is very high in the high mountain zone (zone 4) exceeding 200 kWh/m²/yr; it gradually decreases in zones 3, 2, and 1 to about 180 kWh/m²/yr, 130 kWh/m²/yr, and 70 kWh/m²/yr respectively.

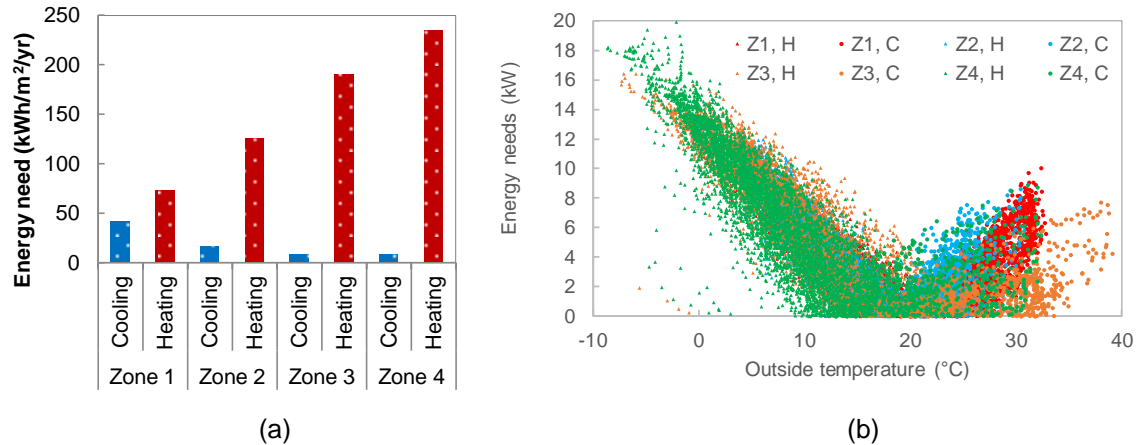


Figure 10- Cooling and heating energy needs per surface unit (a) and energy signature (b) for the base case in the four different climate zones

Energy signature diagrams are widely used for analyzing and predicting buildings' energy use by estimating the cooling and heating energy needs as a function of outdoor temperature. By drawing energy needs with respect to the outside ambient temperature, the energy signatures of the base case in the four different climate zones is obtained and represented in Fig. 10b. The energy signatures for the four climate zones are very similar which confirms that the simulation results are accurate since the energy signature depends mainly on the building design and construction materials and less on the climate conditions. The slope of the heating curve is around 0.88 kW/°C which means that to increase the indoor temperature of the Base Case by 1°C in winter conditions, the required heating energy is 0.88 kW; similarly, the slope of the cooling curve is around 0.8 kW/°C which means that to decrease the indoor temperature of the Base Case by 1°C in summer conditions, the required cooling energy is 0.8 kW.

4.4 Parametric building analysis

The considered parameters that were investigated include: the building orientation and the transparent surfaces' size, the solar absorption level, the air change rate, and the thermal insulation level.

The effect of each parameter on yearly total energy needs was also studied, the remaining parameters being fixed and equal to the ones chosen for the base case. The studied parameters and their variability margin are: the air change rate AC (0.1 – 5 h⁻¹), the walls insulation level W_{ins} (1 – 10 cm), the roof insulation level R_{ins} (1 – 10 cm), the ground floor insulation level G_{ins} (1 – 10 cm), the solar absorptance (0.1 – 0.9), and the windows area in the four directions (2 – 40 m²).

4.4.1 Building orientation and size of the transparent surfaces

Four different openings scenarios were considered (Table 5): the base case scenario, a case having 50% less openings than the base case, a case having 50% more openings than the base case, and a case having 100% more openings than the base case.

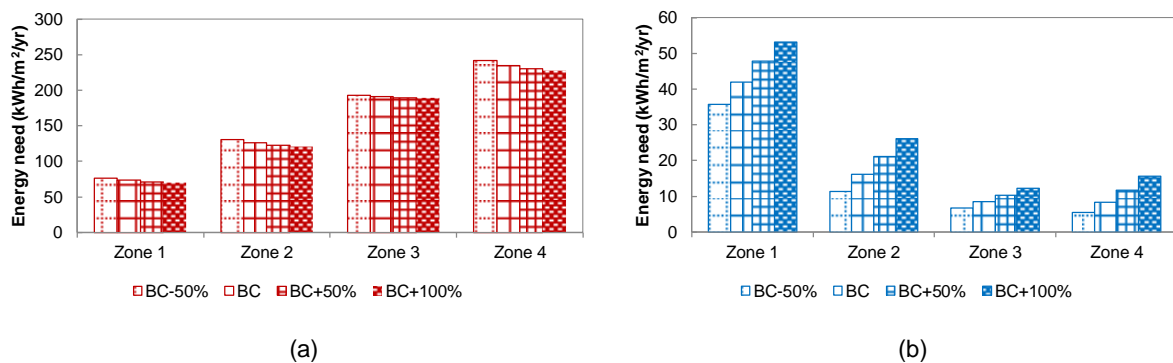
Table 5- Adopted opening areas

Case	Total windows area (m ²)
Base case-50%	15.19
Base case	30.38
Base case+50%	45.57
Base case+100%	60.76

The results of Fig. 11 show that the increase of the glazed surface for the base case allows reducing the heating needs in the four climate zones but causes an increase in cooling energy needs especially in Zone 1 where the increase is about 50% between the smallest and the largest windows area configuration (BC-50% and BC+100%). This can be explained by the effect of solar gains which are beneficial in winter conditions but are considered as additional loads in summer conditions.

In addition to the variation of the openings' size, the effect of the building's orientation on its heating and cooling needs was also investigated. The comparison of the results in Fig. 12 shows that the orientation of the building has a very slight effect on its energy performance.

The results in Table 6 show that the optimal windows area for the Base Case require minimizing the windows area in all directions except for the South direction in the four climate zones. The optimal glazing surface in Zone 1 is 2 m² (minimal value) which is expected since cooling has an important impact in this Zone. In zones 2, 3, and 4, the glazed areas in the South direction are respectively 25, 32, and 40 m² and this is due to the increasing importance of solar gains with respect to the preponderance of heating conditions in the considered climate zone: the more heating is important, the more the window area in the South direction is important. In addition, it can be noticed that the optimal glazed area in the West direction in Zone 4 is about 5 m² and this is also due to the importance of solar gains in this Zone. It is important to highlight that the minimal recommended value for windows area (2 m²) described as an 'extreme case' is only considered from a thermal point of view without considering the day-light factor. In practical scenarios, lighting energy needs should also be considered when recommending the optimal windows area.

**Figure 11- Heating (a) and cooling (b) energy needs for different sizes of transparent surfaces**

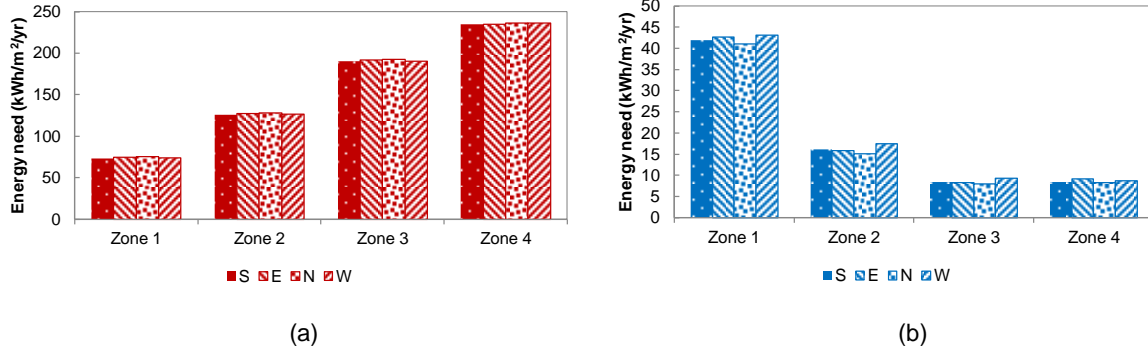


Figure 12- Heating (a) and cooling (b) energy needs for different orientations

Table 6- Optimal windows area in the different directions and for the different climate zones

	Q_{tot}	$A_{win,S}$ (m ²)	$A_{win,W}$ (m ²)	$A_{win,N}$ (m ²)	$A_{win,E}$ (m ²)
Zone 1	16684	2	2	2	2
Zone 2	20998	25.1	2	2	2
Zone 3	29670	32.1	2	2	2
Zone 4	35931	40	4.9	2	2

4.4.2 Solar absorption level

Three different solar absorption coefficient values corresponding to different colors (and textures) of the external opaque envelope surface (walls and roof) were considered: 0.3 (light color), 0.6 (medium color, base case), and 0.9 (dark color) [22,23]. A low solar absorptance allows a better reflection of solar radiations on the opaque building envelope and thus reducing their influence on the building thermal behavior; however, these radiations are beneficial in winter conditions allowing us to get a free additional heating source, but are undesirable in summer. This can be observed in the results of Fig. 13 and for the four climate zones where the lowest solar absorptance (0.3) corresponds to the minimal cooling needs and maximal heating needs while the highest solar absorptance (0.9) corresponds to the minimal heating needs and maximal cooling needs.

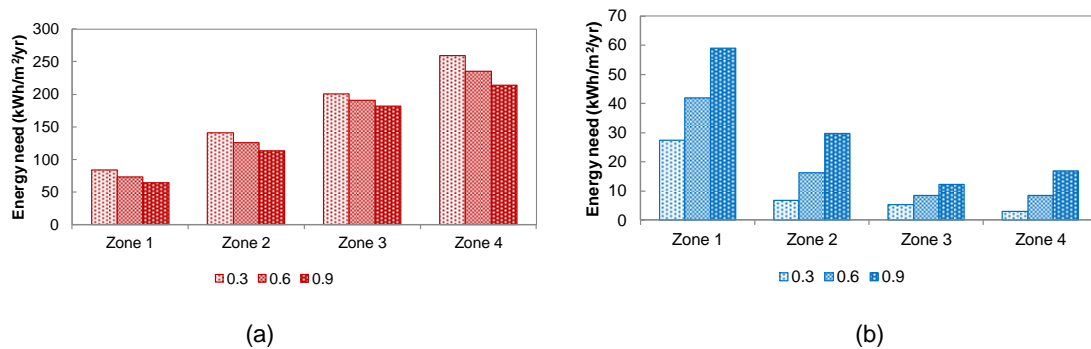


Figure 13- Heating (a) and cooling (b) energy needs for different solar absorption levels of the external surface of the opaque envelope

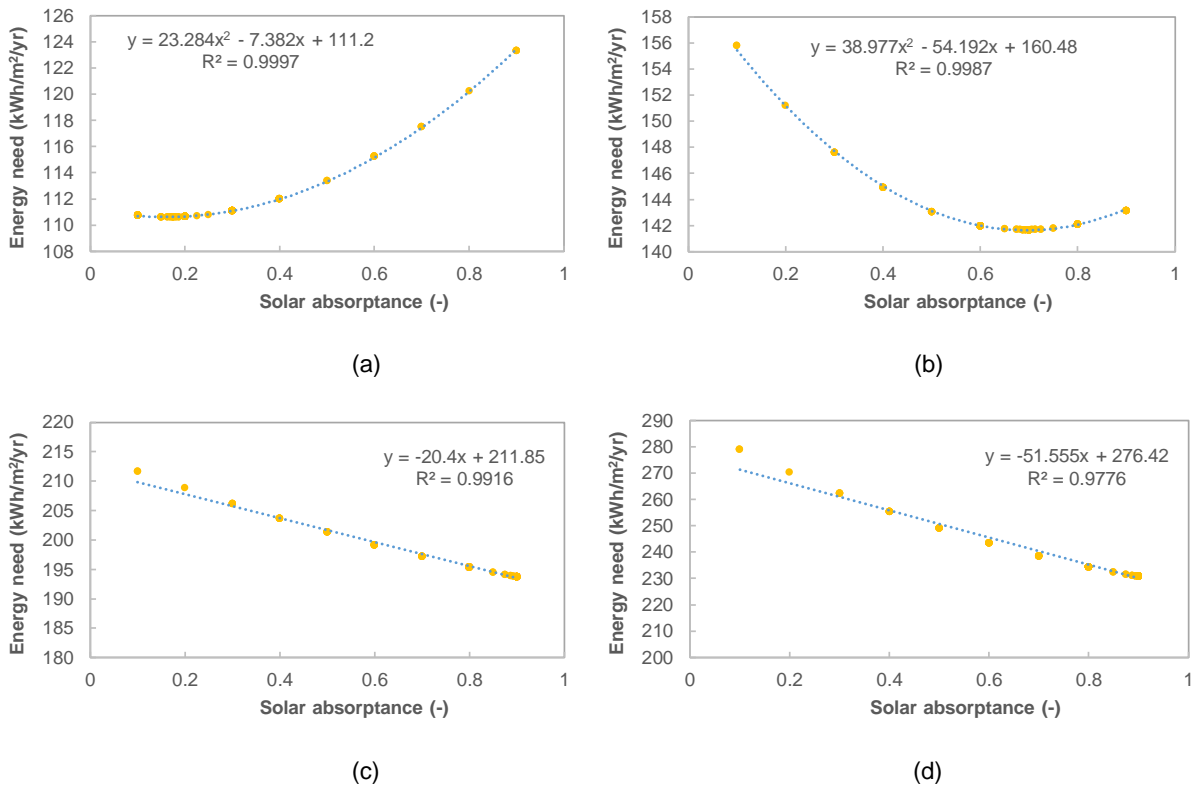


Figure 14- Total energy needs in terms of solar absorptance for climate Zone 1 (a), 2 (b), 3(c) and 4 (d)

The analysis of the optimal solar absorptance varying between 0.1 (reflective surface) and 0.9 (absorbing surface) in the four climate zones in Fig. 14 leads to important conclusions regarding the influence of this parameter in the different zones. In Zone 1, the total yearly energy need curve in terms of the solar absorptance has a parabolic trend with a minimum corresponding to solar absorptance value of 0.175. Below this value, the solar gains are very low leading to an important increase in the heating load and thus an increase in the total energy needs; similarly, beyond this value, the solar gains become important and lead to an increase in cooling load and thus an increase in the total energy needs. In zone 2, the curve has also a parabolic trend and the optimal solar absorptance is 0.694. This value is higher than the value obtained in Zone 1 (0.175) because the heating conditions are more important in this zone and thus the needed solar gains are higher. In zones 3 and 4 the energy needs decrease linearly with the increase of the solar absorptance. In these zones the heating conditions are so important that the solar absorptance should be as high as possible in order to minimize the total energy needs.

4.4.3 Air change rate

The air change rate represents the number of times the air inside a defined space is replaced during one hour; it is equal to the exchanged air volume divided by the space volume. Four typical values for the air change rate were considered: a very tight house with 0.2 air changes per hour, a well-sealed house with 0.5 air changes per hour, a reasonably tight house with an air change rate of about 1 change per hour (base case), and a somewhat older building with no storm windows and caulk missing in spots with an air change rate of 2 changes per hour [24].

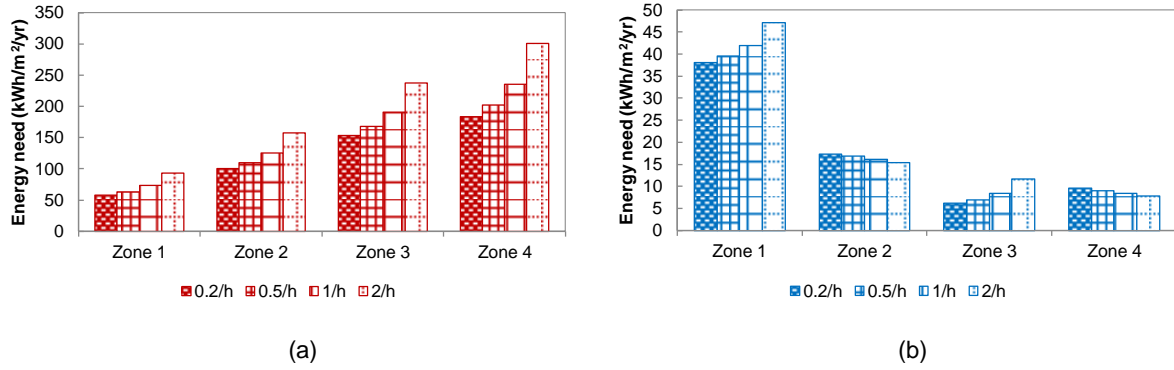


Figure 15- Cooling (a) and heating (b) energy needs for different air change rates

The results of Fig. 15 show that air tightness is a very important factor in winter conditions in the four climate zones while a decrease of about 40% in the heating energy needs is observed between the two extreme cases 2 vol/h and 0.2 vol/h. On the other hand, cooling trends differ between the climate zones; in the coastal zone and inland plateau (zones 1 and 3) the air tightness is recommended for reducing the cooling energy needs, while in the mid-mountain and high-mountain zones (zones 2 and 4) the air tightness the ventilation is rather recommended. This is mainly due to the fact that the outdoor temperature in zones 2 and 4 is lower than the outdoor temperature in zones 1 and 3 and thus natural ventilation seems to be beneficial in these climate conditions.

Fig. 16 shows that the total energy needs increase linearly with the increase of the air change level in the building in the four climate zones. Air tightness is thus a necessity in all climate zones for reaching high levels of building envelope performance.

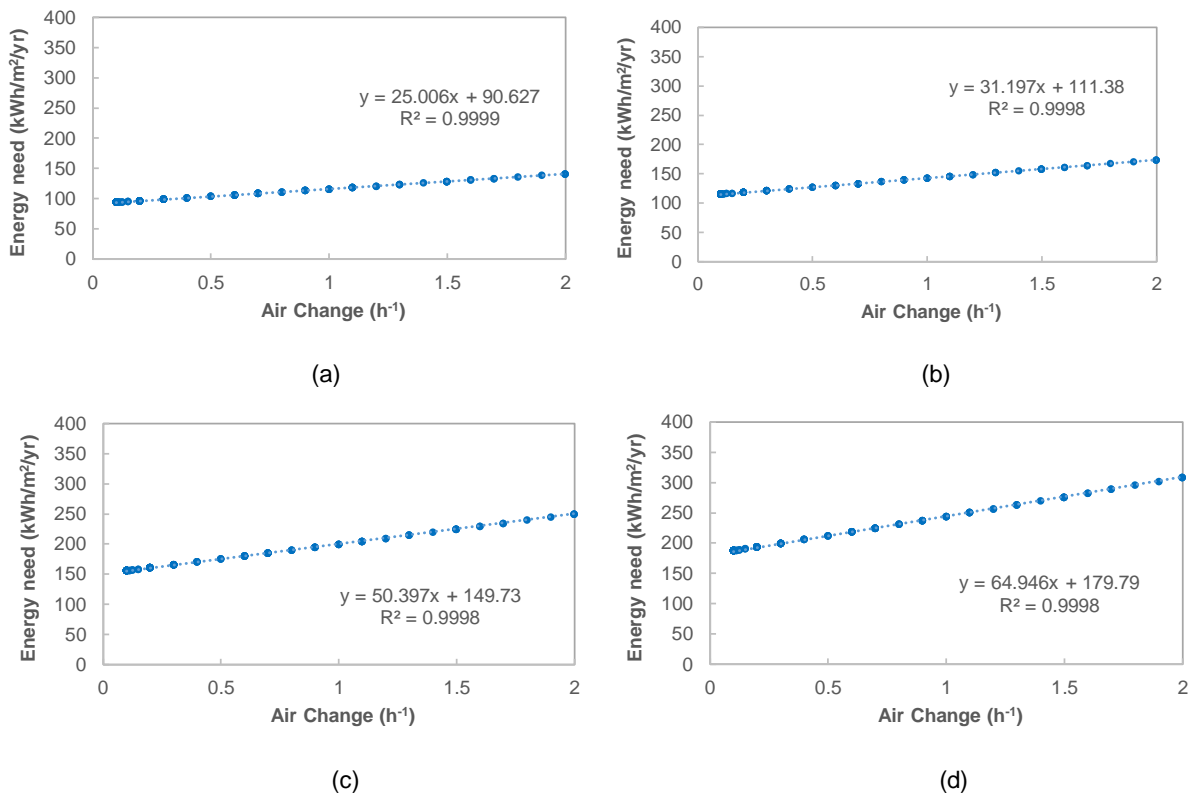


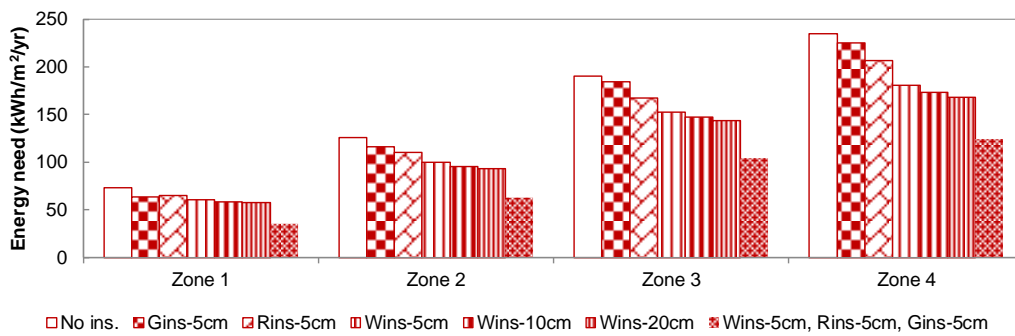
Figure 16- Total energy needs in terms of air change rate for climate Zone 1 (a), 2 (b), 3(c) and 4 (d)

4.4.4 Thermal insulation level

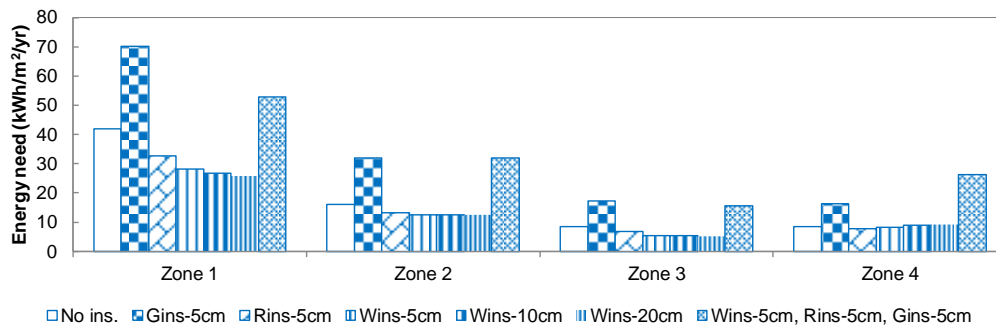
The insulation level of the building envelope allows reducing the conductive heat transfer through the building components and thus reducing the heat transfer from the inside to the outside in winter conditions and from the outside to the inside in summer conditions.

Seven different thermal insulation levels of the opaque envelope were considered in the parametric analysis:

- 1) Uninsulated walls (15 cm hollow block) used in the Base Case and noted as “No ins.”
- 2) Insulated walls with 5 cm of extruded polystyrene and noted as “Wins-5cm”
- 3) Insulated walls with 10 cm of extruded polystyrene and noted as “Wins-10cm”
- 4) Insulated walls with 20 cm of extruded polystyrene and noted as “Wins-20cm”
- 5) Insulated roof with 5 cm of extruded polystyrene and noted as “Rins-5cm”
- 6) Insulated ground floor with 5 cm of extruded polystyrene and noted as “Gins-5cm”
- 7) Insulated walls, roof, and ground floor, with 5 cm of extruded polystyrene and noted as “Wins-5cm, Rins-5cm, Gins-5cm”

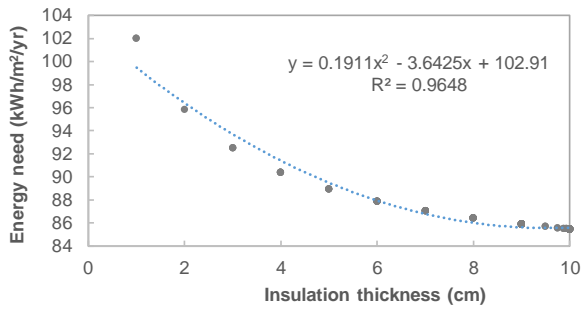


(a)

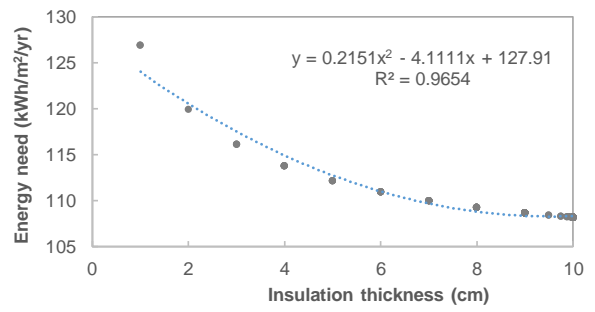


(b)

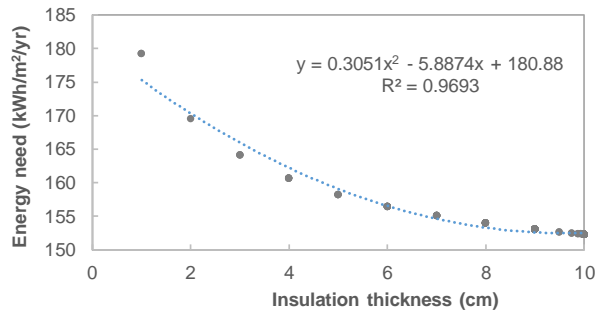
Figure 17- Heating (a) and Cooling (b) energy needs for different insulation levels



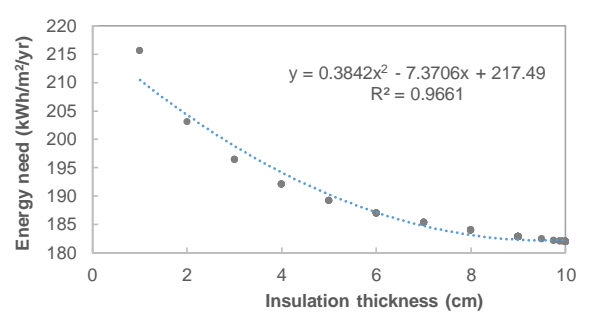
(a)



(b)

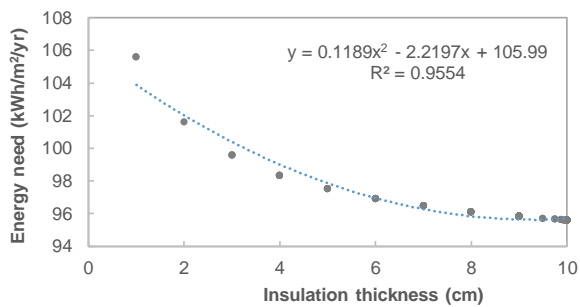


(c)

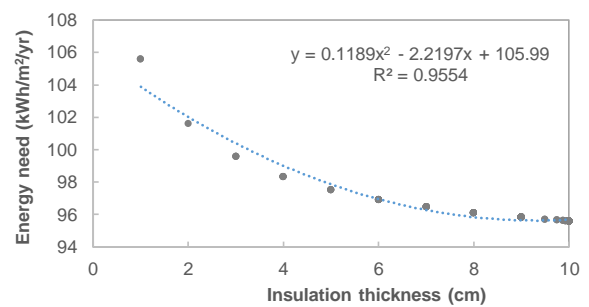


(d)

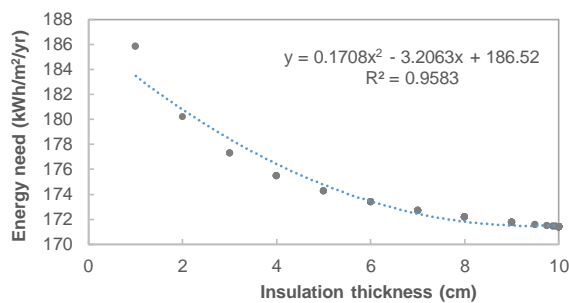
Figure 18- Total energy needs in terms of wall insulation thickness for climate Zone 1 (a), 2 (b), 3 (c) and 4 (d)



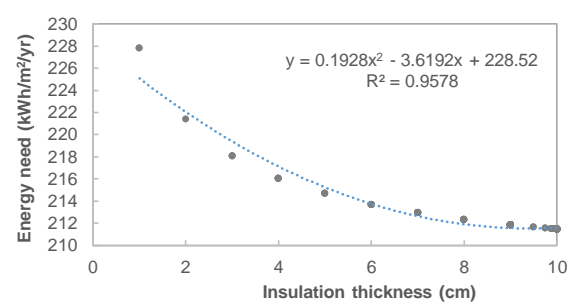
(a)



(b)



(c)



(d)

Figure 19- Total energy needs in terms of roof insulation thickness for climate Zone 1 (a), 2 (b), 3 (c) and 4 (d)

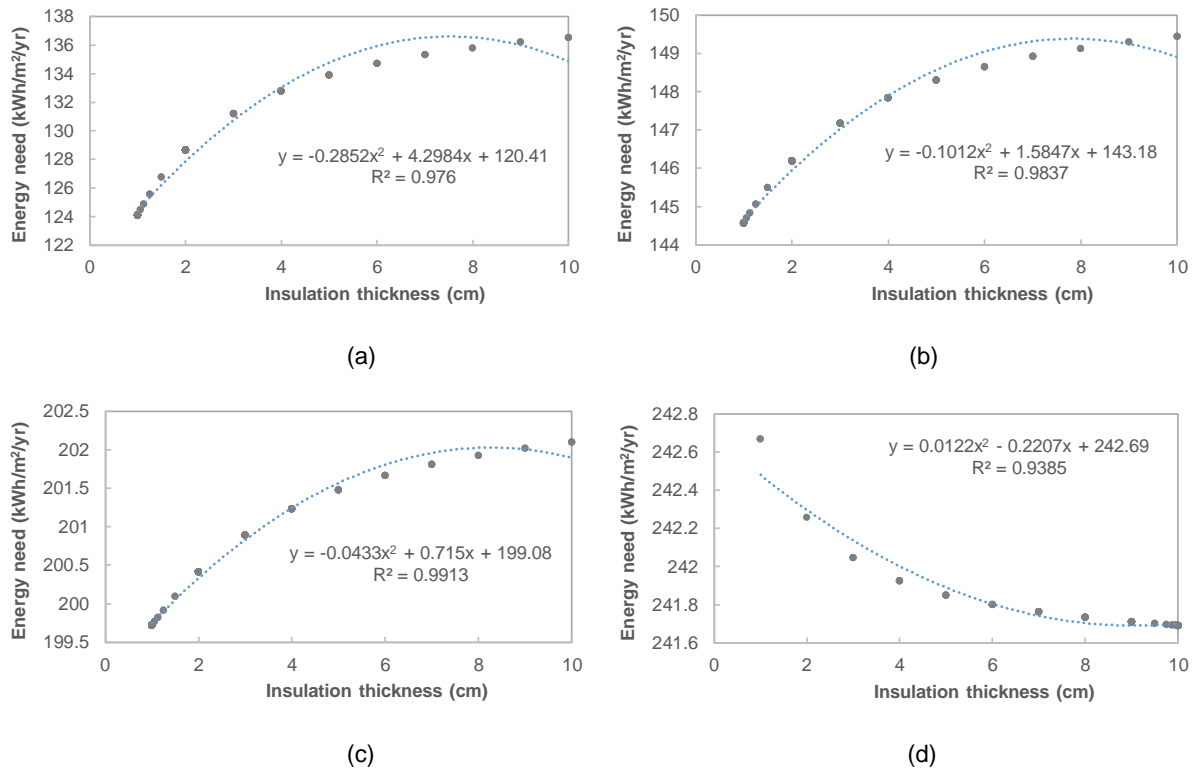


Figure 20- Total energy needs in terms of ground floor insulation thickness for climate Zone 1 (a), 2 (b), 3 (c) and 4 (d)

The impact of ground floor insulation seems to be the least beneficial in heating and has a negative impact on cooling with respect to the base case since the cooling needs increase by adding 5 cm of insulation material to the floor as shown in Fig. 17. Furthermore, the roof and wall insulation present interesting benefits in summer and winter conditions especially in cold climates (zones 3 and 4).

The effect of the insulation level on the building energy performance is represented in Fig. 18 – Fig. 20 for the walls, the roof, and the ground floor respectively.

The wall insulation curves have similar trends in the four climate zones (Fig. 18a – Fig. 18d); the energy need decreases in a parabolic shape and starts stabilizing beyond a thickness of 8 cm. The same conclusions can be drawn by the observations of the roof insulation curves (Fig. 19a – Fig. 19d) where the energy need decreases in a parabolic shape and starts stabilizing beyond a thickness of about 8 cm.

The floor insulation curves in zones 1 and 2 show a parabolic increase (Fig. 20a, and Fig. 20b); the ground floor insulation in these zones is not recommended because it leads to an increase in the energy needs. In zone 3 (Fig.20c) a very slight parabolic increase is observed (around 2 kWh/m²/yr) for the floor insulation; while in zone 4 (Fig. 20d), a very slight parabolic decrease is observed (around 1 kWh/m²/yr) for the floor insulation. This means that the floor insulation in these two zones does not have any noticeable effect.

4.5 Building thermal optimization

Building energy simulations coupled with genetic algorithms has proven its effectiveness for determining the optimum solutions in complex energy efficiency problems taking into account multiple variables; it will thus be used in the present optimization study. After investigating the effect of each parameter separately, a simultaneous optimization is performed for all the parameters for determining the optimal building configuration in the four climate zones. The results of the optimization process in the different climate zones are presented in Table 7. These results show that the optimal energy performance is reached by minimizing the glazed area in all directions, minimizing the air change rate, and maximizing the wall and roof thermal insulation thickness for all the climate zones. The only differences are observed for the Ground floor insulation thickness where a maximal value is required in Zones 3 and 4 and a minimal value is recommended in Zones 1 and 2; and for the solar absorptance which is maximal in Zones 1, 2, and 4 and equal to 0.7 in Zone 2.

Table 7- Optimal building parameters for minimum total energy needs (Heating and Cooling) in the four different climate zones

	Energy need (kWh/m ² /yr)	AC (h ⁻¹)	W_{ins} (cm)	R_{ins} (cm)	G_{ins} (cm)	Solar absorptance (-)	$A_{win,S}$ (m ²)	$A_{win,N}$ (m ²)	$A_{win,E}$ (m ²)	$A_{win,W}$ (m ²)
Zone 1	24.02	0.1	10.0	10.0	0.0	0.9	2	2	2	2
Zone 2	31.73	0.1	10.0	10.0	0.0	0.7	2	2	2	2
Zone 3	40.15	0.1	10.0	10.0	10.0	0.9	2	2	2	2
Zone 4	46.95	0.1	10.0	10.0	10.0	0.9	2	2	2	2

The comparison between the total (cooling and heating) energy needs between the Base Case and the Optimal Case (Fig. 21) shows that substantial thermal improvements of about 80% are observed in the four climate zones.

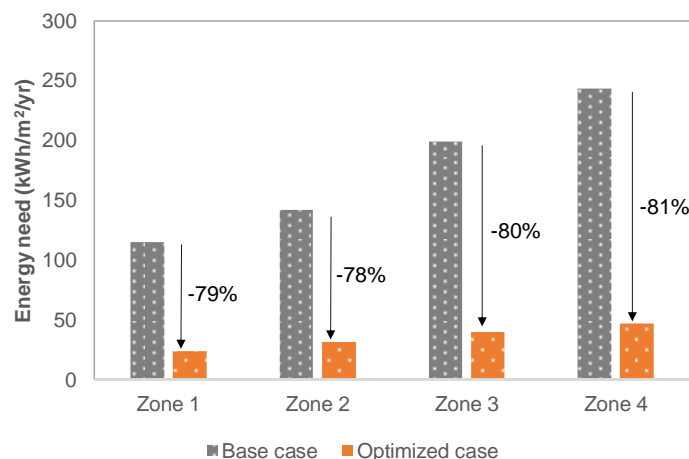


Figure 21- Comparison between the energy needs for the Base Case and the Optimized Case

The optimized parameters shown in table 7 are related to the total energy need (cooling + heating); however, the optimal parameters for heating and/or heating separately are worth to be investigated. In

order to better understand the optimal building parameters for heating and cooling separately, an optimization calculation was performed for cooling only first, then for heating only using the climatic conditions of Zone 1 where heating and cooling are both preponderant. The optimization results in table 8 show that differences between heating and cooling optimal parameters are observed for three parameters:

- The ground floor insulation is maximal for optimal heating needs and minimal for optimal cooling needs.
- The solar absorptance is maximal for optimal heating needs and minimal for optimal cooling needs.
- The glazed area in the South direction is equal to 10.4 m² for optimal heating needs and minimal for optimal cooling needs.

Table 8- Optimal building parameters for minimum Heating and minimum Cooling needs in climate Zone 1

	Energy need (kWh/m ² /yr)	AC (h ⁻¹)	W_{ins} (cm)	R_{ins} (cm)	G_{ins} (cm)	Solar absorptance (-)	$A_{win,S}$ (m ²)	$A_{win,N}$ (m ²)	$A_{win,E}$ (m ²)	$A_{win,W}$ (m ²)
Cooling	0.97	0.1	10	10	1	0.1	2	2	2	2
Heating	8.32	0.1	10	10	10	0.9	10.4	2	2	2

5 Conclusion and recommendations

In the present study, the thermal performance of a Lebanese traditional residential house typology was numerically investigated in the four different Lebanese climate zones. The thermal properties of the building materials of the Lebanese traditional masonry blocks and mortar joints were determined via the guarded hot plates method, and then the equivalent dynamic thermal properties of the masonry wall were computed. A parametric analysis was first performed on a Lebanese traditional detached house typology by examining some parameters having the most effect on the heating and cooling building energy needs: the external climate (climate zone), the building orientation and the transparent surfaces' size, the solar absorption level, the air change rate, and the thermal insulation level. The effects of the different building parameters on the energy needs for space heating and cooling in the different Lebanese climate zones were first analyzed and compared with respect to reference "Base Case" values; the impact of each parameter was evaluated separately on the yearly building total thermal energy needs of the Base Case and was also performed.

Then, a global building optimization investigation was performed by varying all the parameters simultaneously in order to find the best building configuration for optimal yearly energy needs in each climate zone. Some important results and recommendations are summarized as follows:

- Cooling is preponderant in climate zone 1 (coastal zone) with about 60 kWh/m²/yr while in the remaining zones the cooling load is relatively low with less than 20 kWh/m²/yr and can thus be neglected with respect to space heating by preserving an indoor temperature less than 28°C.
- Heating load is very high in zone 4 exceeding 250 kWh/m²/yr; it gradually decreases in zones 3, 2, and 1 to about 220 kWh/m²/yr, 140 kWh/m²/yr, and 70 kWh/m²/yr respectively.

- The optimal energy performance is reached by minimizing the glazed area in all directions, minimizing the air change rate, and maximizing the wall and roof thermal insulation thickness for all the climate zones. The only differences are observed for the Ground floor insulation thickness where a maximal value is required in Zones 3 and 4 and a minimal value is recommended in Zones 1 and 2; and for the solar absorptance which is maximal in Zones 1, 2, and 4 and equal to 0.7 in Zone 2.
- Substantial thermal improvements of about 80% between the Base Case and the Optimal Case can be obtained in the four climate zones.

To sum up, this study improves the knowledge and provides a scientific comprehensive understanding of the thermal performance of residential houses in Mediterranean climate conditions by investigating the thermal performance of a Lebanese traditional house in the four Lebanese climate zones. The findings of this work can be applied for new buildings as guidelines for optimal efficient design as well as in existing buildings because the determination of the best interventions and the potential savings is primordial for any eventual thermal improvement of the envelope. The conformity of the new designs with obtained results can improve comfort, and reduce the energy needs in this category of buildings. The obtained results from this case study can be extended to similar buildings having a similar geometry and located in similar climate conditions. More simulations and building scenarios need to be performed on collective residential buildings and other building typologies to generalize the findings.

Conflict of Interests

The authors declare no conflict of interests regarding the publication of this paper.

References

- [1] M. Melanie, *An Introduction to Genetic Algorithms*, MIT Press, 1999, doi: 10.1016/S0898-1221(96)90227-8.
- [2] F. Salata, V. Ciancio, J. Dell'Olmo, I. Golasi, O. Palusci, M. Coppi, "Effects of local conditions on the multi-variable and multi-objective energy optimization of residential buildings using genetic algorithms", *Applied Energy*, vol. 260, 114289, (2020), DOI: 10.1016/j.apenergy.2019.114289
- [3] S. Bucking, R. Zmeureanu, A. Athienitis, "A methodology for identifying the influence of design variations on building energy performance", *Journal of Building Performance Simulation*, vol. 7, issue 6, pp. 411-426, (2014), DOI: 10.1080/19401493.2013.863383
- [4] K. M. S. Chvatal, H. Corvacho, "The impact of increasing the building envelope insulation upon the risk of overheating in summer and an increased energy consumption", *Journal of Building Performance Simulation*, vol. 2, issue 4, pp. 267-282, (2009), DOI: 10.1080/19401490903095865
- [5] M. Ibrahim, N. Ghaddar, K. Ghali, "Optimal location and thickness of insulation layers for minimizing building energy consumption", *Journal of Building Performance Simulation*, vol. 5, issue 6, pp. 384-398, (2012), DOI: 10.1080/19401493.2012.657686
- [6] J. Jin, J. Jeong, "Optimization of a free-form building shape to minimize external thermal load using genetic algorithm", *Energy and Buildings*, vol. 85, pp. 473–482, (2014), DOI: 10.1016/j.enbuild.2014.09.080
- [7] F. Rosso, V. Ciancio, J. Dell'Olmo, F. Salata, "Multi-objective optimization of building retrofit in the Mediterranean climate by means of genetic algorithm application", *Energy & Buildings*, vol. 216, 109945, (2020), DOI: 10.1016/j.enbuild.2020.109945

- [8] J. A. Wright, A. Brownlee, M. M. Mourshed, M. O. Wang, "Multi-objective optimization of cellular fenestration by an evolutionary algorithm", *Journal of Building Performance Simulation*, vol. 7, issue 1, pp. 33-51, (2014), DOI: 10.1080/19401493.2012.762808
- [9] A. Zhang, R. Bokel, A. Dobbelsteen, Y. Sun, Q. Huang, Q. Zhang, "Optimization of thermal and daylight performance of school buildings based on a multi-objective genetic algorithm in the cold climate of China", *Energy and Buildings*, vol. 139, pp. 371-384, (2017), DOI: 10.1016/j.enbuild.2017.01.048
- [10] World Bank, "Energy efficiency study in Lebanon", December 2009
- [11] ALMEE, "Thermal Standards for Buildings in Lebanon", TSBL 2010
- [12] E. H. El Andaloussi, R. Missaoui, A. Mourtada, S. Pouffary, A. Roza "Energie, changement climatique et bâtiment en Méditerranée : perspectives régionales", Plan Bleu, Centre d'activités régionales, PNUE-PAM, Sophia Antipolis, June 2010
- [13] Solar Energy Laboratory, 2002. TRNSYS version 16. Wisconsin, USA: Solar Energy Laboratory
- [14] Sassine, E., Cherif, Y., Dgheim, J. et al. "Experimental and Numerical Thermal Assessment of Lebanese Traditional Hollow Blocks". *Int J Thermophys* 41, 47 (2020), DOI: 10.1007/s10765-020-02626-7
- [15] Lebanese Agricultural Research Institute, <http://www.lari.gov.lb/>.
- [16] B. Dong, D. Yan, Z. Li, Y. Jin, X. Feng, H. Fontenot, "Modeling occupancy and behavior for better building design and operation—A critical review", *Building Simulation*, vol. 11, pp. 899–921, (2018)
- [17] E. Cuerda, O. Guerra-Santin, J. J. Sendra & Fco. J. N. González, "Comparing the impact of presence patterns on energy demand in residential buildings using measured data and simulation models", *Building Simulation*, vol. 12, pp. 985–998, (2019)
- [18] Y. Chen, T. Hong, X. Luo, "An agent-based stochastic Occupancy Simulator", *Building Simulation*, vol. 11, pp. 37–49, (2018)
- [19] A. Muroi, I. Gaetani, P. Hoes, J. L. M. Hensen, "Occupant behavior in identical residential buildings: A case study for occupancy profiles extraction and application to building performance simulation", *Building Simulation*, vol. 12, pp. 1047–1061, (2019)
- [20] AgriMetSoft (2019). Online Calculators. Available on:
<https://agrimetsoft.com/calculators/Nash%20Sutcliffe%20model%20Efficiency%20coefficient>
- [21] ANSI/ASHRAE Standard 55, "Thermal Environmental Conditions For Human Occupancy" 2017.
- [22] M. Alpuche, I. González, J. Ochoa, I. Marincic, A. Duarte, E. Valdenebro, "Influence of absorptance in the building envelope of affordable housing in warm dry climates", *Energy Procedia* 57 (2014) pp. 1842 – 1850, (2013), DOI: 10.1016/j.egypro.2014.10.048
- [23] K. Dornelles, V. Roriz, M. Roriz, "Determination of the solar absorptance of opaque surfaces", PLEA2007 - The 24th Conference on Passive and Low Energy Architecture, Singapore, 22-24 November 2007, DOI: 10.13140/RG.2.1.2368.1764
- [24] C. Younes, C. Abi Shdid, G. Bitsuamlak, "Air infiltration through building envelopes: A review", *Journal of Building Physics*, vol. 35, (2012), DOI: 10.1177/1744259111423085